

General Relativity Resolves Galactic Rotation Without Exotic Dark Matter

F. I. Cooperstock and S. Tieu

Department of Physics and Astronomy, University of Victoria

P.O. Box 3055, Victoria, B.C. V8W 3P6 (Canada)

e-mail addresses: cooperstock@phys.uvic.ca, stieu@uvic.ca

Abstract

A galaxy is modeled as a stationary axially symmetric pressure-free fluid in general relativity. For the weak gravitational fields under consideration, the field equations and the equations of motion ultimately lead to one linear and one non-linear equation relating the angular velocity to the fluid density. It is shown that the rotation curves for the Milky Way, NGC 3031, NGC 3198 and NGC 7331 are consistent with the mass density distributions of the visible matter concentrated in flattened disks. Thus the need for a massive halo of exotic dark matter is removed. For these galaxies we determine the mass density for the luminous threshold as $10^{-21.75} \text{ kg}\cdot\text{m}^{-3}$.

Subject headings: galaxies: kinematics and dynamics-gravitation-relativity-dark matter

1 Introduction

The problem of accounting for the observed essentially flat galactic rotation curves has been a central issue in astrophysics. There has been much speculation over the question

of the nature of the dark matter that is believed to be required for the consistency of the observations with Newtonian gravitational theory. Clearly the issue is of paramount importance given that the dark matter is said to constitute the dominant constituent of a galactic mass [1]. The dark matter enigma has served as a spur for particle theorists to devise acceptable candidates for its constitution. While physicists and astrophysicists have pondered over the issue, other researchers have devised new theories of gravity to account for the observations (see for example [3]). However the latter approaches, imaginative as they may be, have met with understandable skepticism, having been devised solely for the purpose of the task at hand. General relativity remains the preferred theory of gravity with Newtonian theory as its limit. General relativity has been successful in every test that it has encountered, going beyond Newtonian theory where required.

It is understandable that the conventional gravity approach has focused upon Newtonian theory in the study of galactic dynamics as the galactic field is weak (apart from the deep core regions where black holes are said to reside) and the motions are non-relativistic ($v \ll c$). It was this approach that led to the inconsistency between the theoretical Newtonian-based predictions and the observations of the visible sources. To reconcile the theory with the observations, researchers subsequently concluded that dark matter must be present around galaxies in vast massive halos that constitute the great bulk of the galactic masses ¹. However, in dismissing general relativity in favor of Newtonian gravitational theory for the study of galactic dynamics, insufficient attention has been paid to the fact that the stars that compose the galaxies are essentially in motion under gravity alone (“gravitationally bound”). It has been known since the time of Ed-

¹See however [4] who argues for a much less massive halo based upon gravitational lensing data.

dington that the gravitationally bound problem in general relativity is an intrinsically non-linear problem even when the conditions are such that the field is weak and the motions are non-relativistic, at least in the time-dependent case. *Most significantly, we have found that under these conditions, the general relativistic analysis of the problem is also non-linear for the stationary (non-time-dependent) case at hand.* Thus the intrinsically linear Newtonian-based approach used to this point has been inadequate for the description of the galactic dynamics and Einstein’s general relativity should be brought into the analysis within the framework of established gravitational theory². This is an essential departure from conventional thinking on the subject and it leads to major consequences as we discuss in what follows. We will demonstrate that via general relativity, the generating potentials producing the observed flattened galactic rotation curves are necessarily linked to the mass density distributions of the flattened disks, obviating any necessity for dark matter halos in the total galactic composition. We will also present the indicator that the threshold for luminosity occurs at a density of $10^{-21.75} \text{ kg}\cdot\text{m}^{-3}$.

2 The Model Galaxy

Within the context of Newtonian theory, Mestel [2] considered a special rotating disk with surface density inversely proportional to radius. Using a disk potential with Bessel functions that we will also use in what follows but in quite a different manner, he found

²Actually within the framework of Newtonian theory, it is possible to define an “effective” potential (see for example [1] page 136) to incorporate the centrifugal acceleration in a rotating coordinate system with a given angular velocity. Since this contains the square of the angular velocity of the rotating frame, there is already the hint of non-linearity present. However, in what follows in general relativity, we will see the non-linearity related to the angular velocity as a *variable* function. Moreover, for a system in rotation, this non-linearity cannot be removed globally.

that it leads to an absolutely flat galactic rotation velocity curve.³ Interestingly, the gradient of the potential in this, as in all Newtonian treatments, relates to acceleration whereas in the general relativistic treatment, we will show that the gradient of a “generating potential” gives the tangential velocity (15).

To model a galaxy in its simplest form in terms of its essential characteristics, we consider a uniformly rotating fluid without pressure and symmetric about its axis of rotation. We do so within the context of general relativity. The stationary axially symmetric metric can be described in generality in the form

$$ds^2 = -e^{\nu-w}(udz^2 + dr^2) - r^2e^{-w}d\phi^2 + e^w(cdt - Nd\phi)^2 \quad (1)$$

where u , ν , w and N are functions of cylindrical polar coordinates r , z . It is easy to show that to the order required, u can be taken to be unity. It is most simple to work in the frame that is co-moving with the matter

$$U^i = \delta_0^i \quad (2)$$

where U^i is the 4-velocity⁴. This was done in the pioneering paper by van Stockum [6] who set $w = 0$ from the outset⁵. As in [7], we perform a purely *local* (r , z held fixed) transformation

$$\bar{\phi} = \phi + \omega(r, z) t \quad (3)$$

that locally diagonalizes the metric. In this manner, we are able to deduce the local

³This is also the case for the MOND [3] model.

⁴This is reminiscent of the standard approach that is followed for FRW cosmologies. However, the FRW spacetimes are homogeneous and they are not stationary

⁵Interestingly, the geodesic equations imply that $w = \text{constant}$ (which can be taken to be zero as in [6]) even for the *exact* Einstein field equations as studied in [6] (see (8) and (9)).

angular velocity ω and the tangential velocity V as

$$\omega = \frac{Nce^w}{r^2e^{-w} - N^2e^w} \approx \frac{Nc}{r^2},$$

$$V = \omega r$$
(4)

with the approximate value applicable for the weak fields under consideration. The Einstein field equations to order G are⁶

$$\begin{aligned} 2r\nu_r + N_r^2 - N_z^2 &= 0, \\ r\nu_z + N_r N_z &= 0, \\ N_r^2 + N_z^2 + 2r^2(\nu_{rr} + \nu_{zz}) &= 0, \\ N_{rr} + N_{zz} - \frac{N_r}{r} &= 0, \\ \left(w_{rr} + w_{zz} + \frac{w_r}{r}\right) + \frac{3}{4}r^{-2}(N_r^2 + N_z^2) \\ + Nr^{-2} \left(N_{rr} + N_{zz} - \frac{N_r}{r}\right) - \frac{1}{2}(\nu_{rr} + \nu_{zz}) &= \frac{8\pi G\rho}{c^2} \end{aligned}$$
(5)

where G is the gravitational constant and ρ is the mass density. Subscripts denote partial differentiation with respect to the indicated variable. These equations are easily combined to yield

$$\nabla^2 w + \frac{N_r^2 + N_z^2}{r^2} = \frac{8\pi G\rho}{c^2}$$
(6)

where

$$\nabla^2 w \equiv w_{rr} + w_{zz} + \frac{w_r}{r}$$
(7)

and ν would be determined by quadratures. Since the pressure-free fluid elements must satisfy the geodesic equation as their equation of motion

$$\frac{dU^i}{ds} + \Gamma_{kl}^i U^k U^l = 0$$
(8)

⁶This is a loose notation favored by many relativists but adequate for our purposes here as a smallness parameter.

we find using (1) and (2) that

$$w_r = w_z = 0 \quad (9)$$

and hence

$$\nabla^2 w = 0 \quad (10)$$

within the fluid⁷. It is to be noted that it is the *freely gravitating motion* of the source material (the stars) in conjunction with the choice of co-moving coordinates (2) that leads to the constancy of w within the source. Had there been pressure, w would have been variable⁸. With this freely gravitating constraint, the interior field equations for N and ρ are reduced to

$$N_{rr} + N_{zz} - \frac{N_r}{r} = 0 \quad (11)$$

$$\frac{N_r^2 + N_z^2}{r^2} = \frac{8\pi G\rho}{c^2} \quad (12)$$

Note that from both the field equation for ρ and the expression for ω that N is of order $G^{1/2}$. The non-linearity of the galactic dynamical problem is manifest through the non-linear relation⁹ between the functions ρ and N . Rotation under freely gravitating motion is the key here. By contrast, for time-independence in the non-rotating problem, there must be pressure present to maintain a static configuration, N vanishes for vanishing ω

⁷Normally, the fall-off of w with $R \equiv \sqrt{r^2 + z^2}$ is used to derive the total mass of an isolated system. However, w is constant in this system of coordinates by (9) and we cannot do so here. The w constancy does not imply that the mass is zero. In other (non-co-moving) coordinate systems, w would be seen to be variable. With the field being weak and the system being non-relativistic, the mass is well-approximated simply by the integral of ρ over *coordinate* volume. Moreover, we will choose solutions that are free of singularities and hence free of the ambiguities present in [7].

⁸Even in freely gravitating motion, w would have been variable had we opted for non-co-moving coordinates.

⁹While we have eliminated w using (8) to get (12) by choice of co-moving coordinates, N cannot be eliminated and hence non-linearity is intrinsic to the study of the galactic dynamics.

and $\nabla^2 w$ is non-zero yielding the familiar Poisson equation of Newtonian gravity. In the present case, it is the *rotation* via the function N that connects directly to the density and the now non-linear equation is in sharp contrast to the linear Poisson equation. Interestingly, (11) can be expressed as

$$\nabla^2 \Phi = 0 \tag{13}$$

where

$$\Phi \equiv \int \frac{N}{r} dr \tag{14}$$

and hence flat-space harmonic functions Φ are the generators of the axially symmetric stationary pressure-free weak fields that we seek¹⁰. Using (4) and (14), we have the expression for the tangential velocity of the distribution

$$\begin{aligned} V &= c \frac{N}{r} \\ &= c \frac{\partial \Phi}{\partial r} \end{aligned} \tag{15}$$

3 Modeling the Observed Galactic Rotation Curves

Since the field equation for ρ is non-linear, the simpler way to proceed in galactic modeling is to first find the required generating potential Φ and from this, derive an appropriate function N for the galaxy that is being analyzed. With N found, (12) yields the density distribution. If this is in accord with observations, the efficacy of the approach is established. Every galaxy is different and each requires its own composing elements to build the generating potential. In cylindrical polar coordinates, separation of variables

¹⁰In fact Winicour [5] has shown that all such sources, even when the fields are strong, are generated by such flat-space harmonic functions.

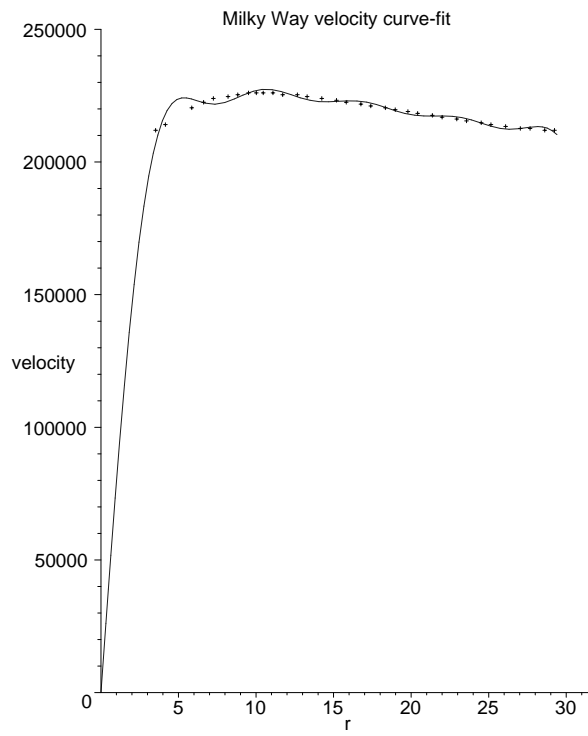


Figure 1: Velocity curve-fit for the Milky Way in units of m/s vs Kpc.

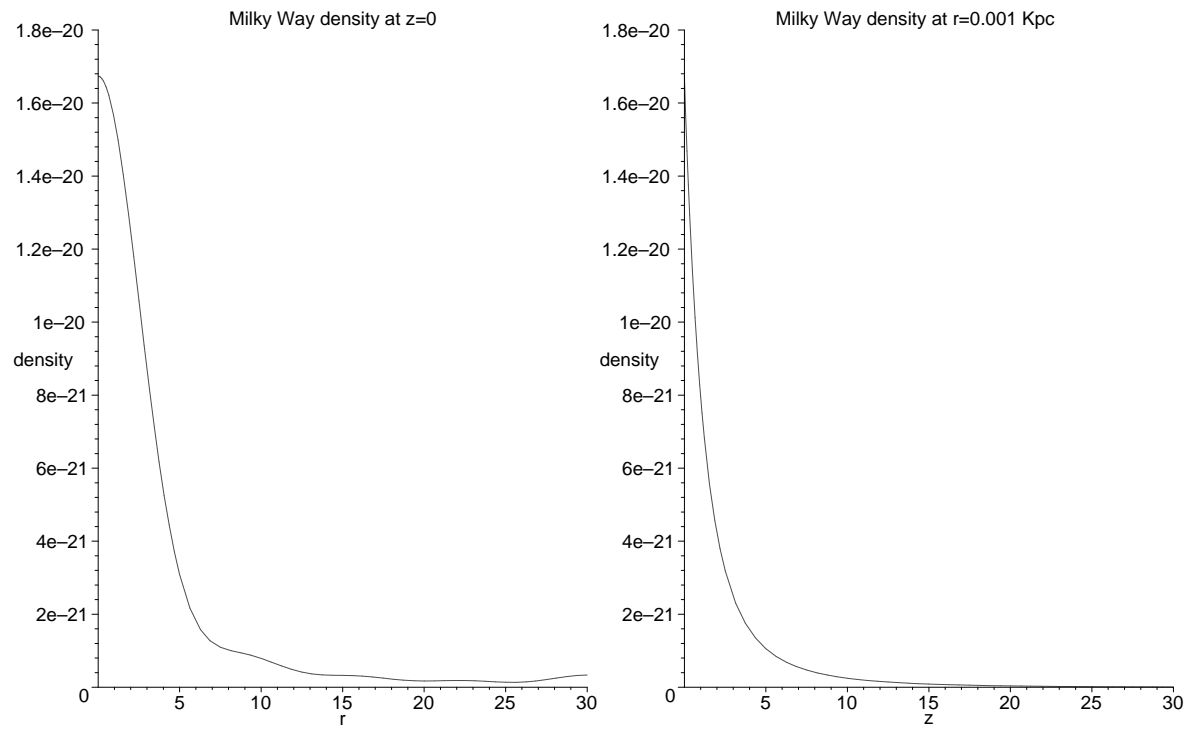


Figure 2: Derived density profiles in units of kg/m^3 for the Milky Way at $z = 0$ (left) and $r = 0.001$ Kpc (right).

yields the following solution for Φ in (13):

$$\Phi = Ce^{-k|z|}J_0(kr) \quad (16)$$

where J_0 is the Bessel function $n = 0$ of Bessel $J_n(kr)$ and C is an arbitrary constant.

¹¹ We use the linearity of (13) to express the general solution of this form as a linear superposition

$$\Phi = \sum_n C_n e^{-k_n|z|} J_0(k_n r) \quad (17)$$

with n chosen appropriately for the desired level of accuracy. From (17) and (4), the tangential velocity ¹² is

$$V = -c \sum_n k_n C_n e^{-k_n|z|} J_1(k_n r) \quad (18)$$

With the k_n chosen so that the $J_0(k_n r)$ terms are orthogonal ¹³ to each other, we have found that only 10 functions with parameters C_n , $n \in \{1 \dots 10\}$ suffice to provide an excellent fit¹⁴ to the velocity curve for the Milky Way. The details are provided in

¹¹The absolute value of z must be used to provide the proper reflection of the distribution for negative z . While this produces a discontinuity in N_z at $z = 0$, it is important to note that this has no physical consequence since N_z enters as a square in the density and N_z does not play a role in the equations of motion. Moreover, the metric itself is continuous. This is analogous to the Schwarzschild constant density sphere problem that leads to a discontinuity in metric derivative across the matter-vacuum interface in Schwarzschild coordinates. In principle, other coordinates could be found to render the metric and its first partial derivatives globally continuous but this would be counter-productive as it would unnecessarily complicate the mathematics. As in FRW, our co-moving coordinates simplify the analysis.

¹² $dJ_0(x)/dx = -J_1(x)$ from [8].

¹³Just as the $\sin kx$ functions are orthogonal for integer k , the Bessel functions $J_0(kr)$ have their own orthogonality relation: $\int_0^1 J_0(k_n r) J_0(k_m r) r dr \propto \delta_{mn}$ where k_n are the zeros of J_0 at the limits of integration. This orthogonality condition is on Φ rather than on V because the differential equation dictates the integral condition.

¹⁴It should be noted that unlike typical velocity curve fits that allow arbitrary velocity functions, our curve fits are constrained by the demand that they be created from derivatives of harmonic functions.

the Appendix and the curve fit is shown in Figure 1. ¹⁵ From (15) and (18), the N function is determined in detail and from (12), the density distribution. This is shown in Figure 2 as a function of r at $z = 0$ as well as a function of z at $r = 0.001$ Kpc. We see that the distribution is a flattened disk with good correlation with the observed density data for the Milky Way. The integrated mass is found to be $21 \times 10^{10} M_{\odot}$ which is at the lower end of the estimated mass range of $20 \times 10^{10} M_{\odot}$ to $60 \times 10^{10} M_{\odot}$ as established by various researchers. It is to be noted that the approximation scheme would break down in the region of the galactic core should the core harbor a black hole or even a naked singularity (see e.g. [12]). *Most significantly, our correlation of the flat velocity curve is achieved with disk mass of an order of magnitude smaller than the envisaged halo mass of exotic dark matter.* (See e.g. [13] for proposed values of extended halo masses.) General relativity does not distinguish between the luminous and non-luminous contributions. The ρ density distribution deduced is derived from the totality of the two. Any substantial amount of non-luminous matter would necessarily lie in the flattened region close to $z = 0$ because this is the region of significant ρ and would be due to dead stars, planets, neutron stars and other normal baryonic matter debris. Each term within the series has z -dependence of $e^{-k_n|z|}$ which causes the steep density fall-off profile as shown in Figure 2(b). This fortifies the picture of a standard galactic disk-like shape as opposed to a halo sphere. From the evidence provided by rotation curves, there is no support for the widely accepted notion of massive halos of

¹⁵Note that the $J_1(x)$ Bessel functions are 0 at $x = 0$ and oscillate with decreasing amplitude, falling as $1/\sqrt{x}$ asymptotically [8], as desired for merging with Keplerian behavior at infinity. Also, the present curves drop as r approaches 0. This is in contrast to the Mestel [2] and MOND [3] curves that are flat everywhere.

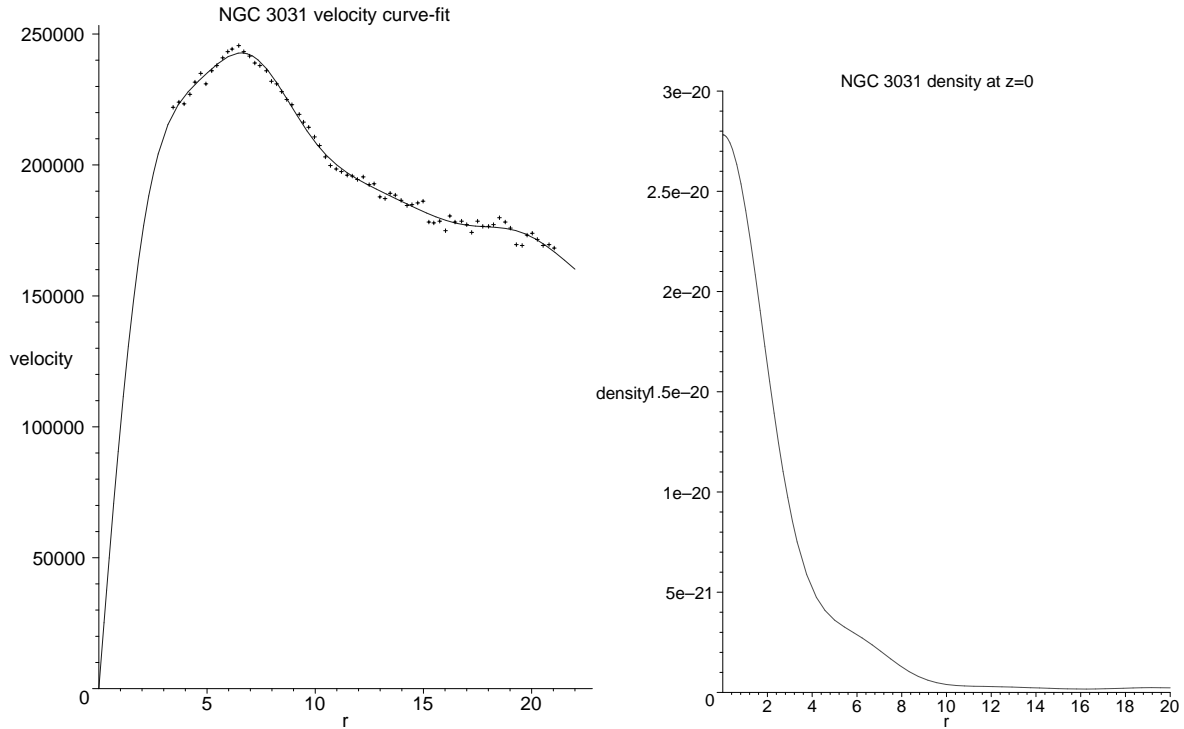


Figure 3: Velocity curve-fit and derived density for NGC 3031

exotic dark matter surrounding visible galactic disks: conventional gravitational theory, namely general relativity, accounts for the observed flat galactic rotation curves linked to flattened disks with no exotic dark matter.

We have also performed curve fits for the galaxies NGC 3031, NGC 3198 and NGC 7331. The data are provided in the Appendix and the remarkably precise velocity curve fits are shown in Figures 3 to 5 where the density profiles are presented for r at $z = 0$. Again the picture is consistent with the observations and the mass is found to be $10.1 \times 10^{10} M_{\odot}$ for NGC 3198. This can be compared to the result from Milgrom's [3] modified Newtonian dynamics of $4.9 \times 10^{10} M_{\odot}$ and the value given through observations

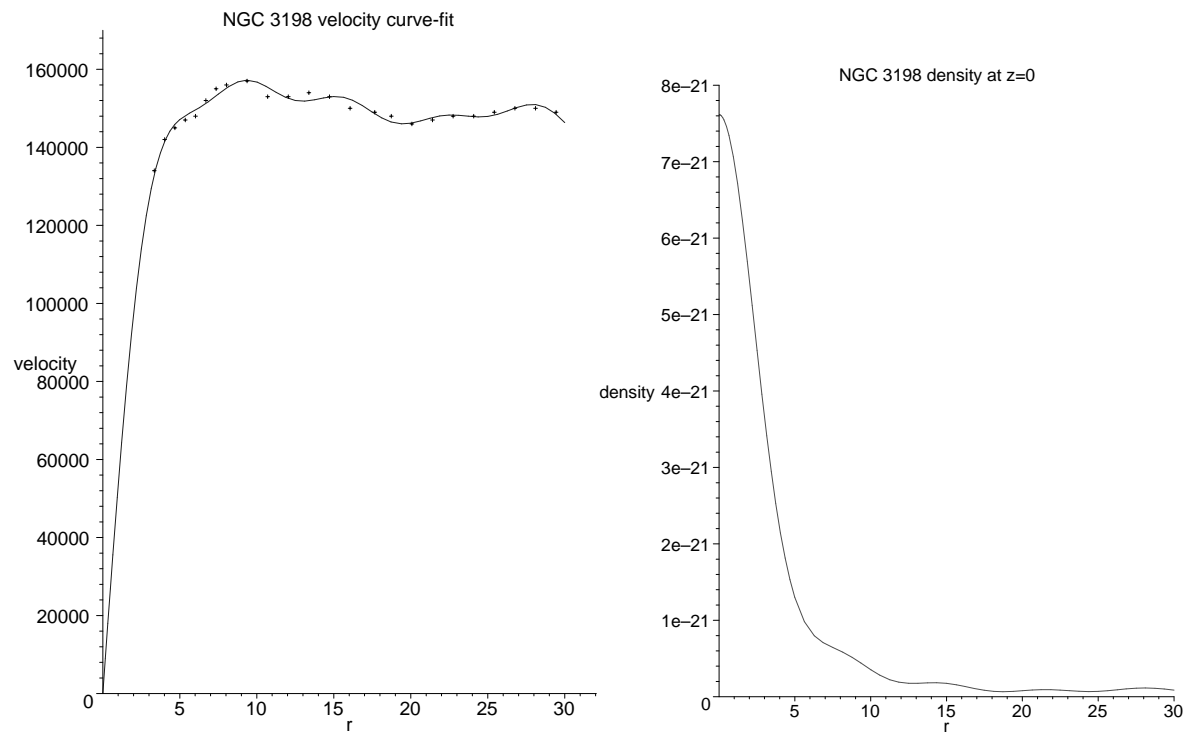


Figure 4: Velocity curve-fit and derived density for NGC 3198

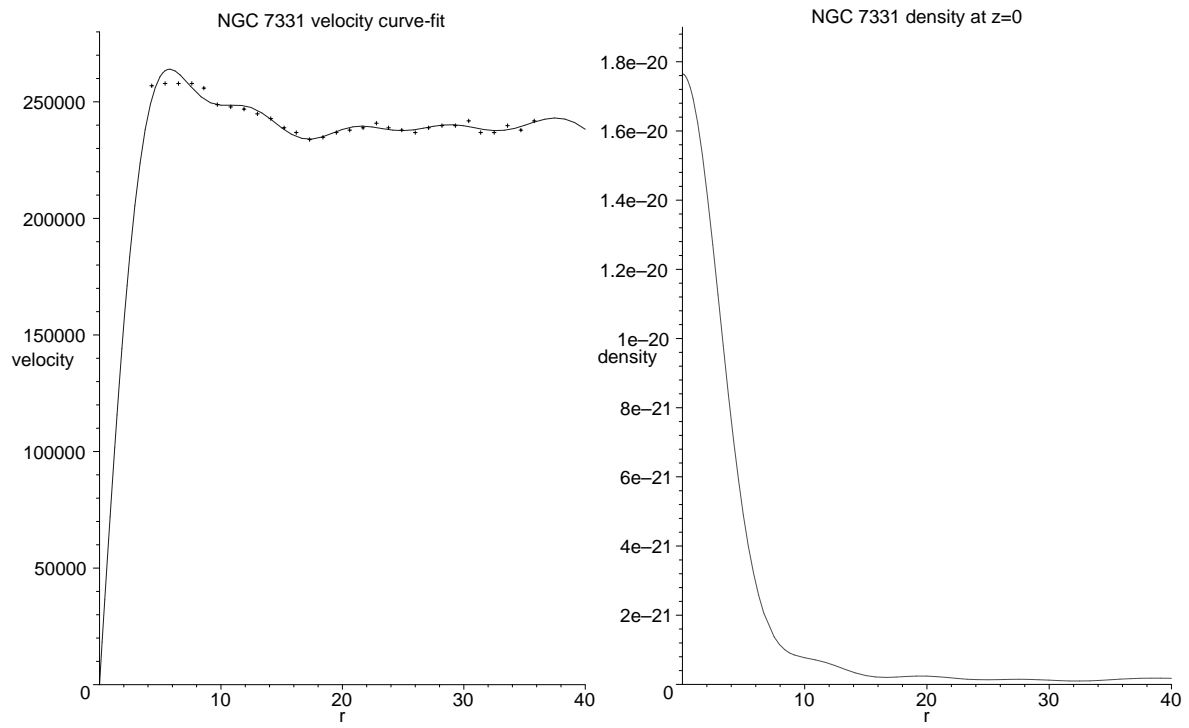


Figure 5: Velocity curve-fit and derived density for NGC 7331

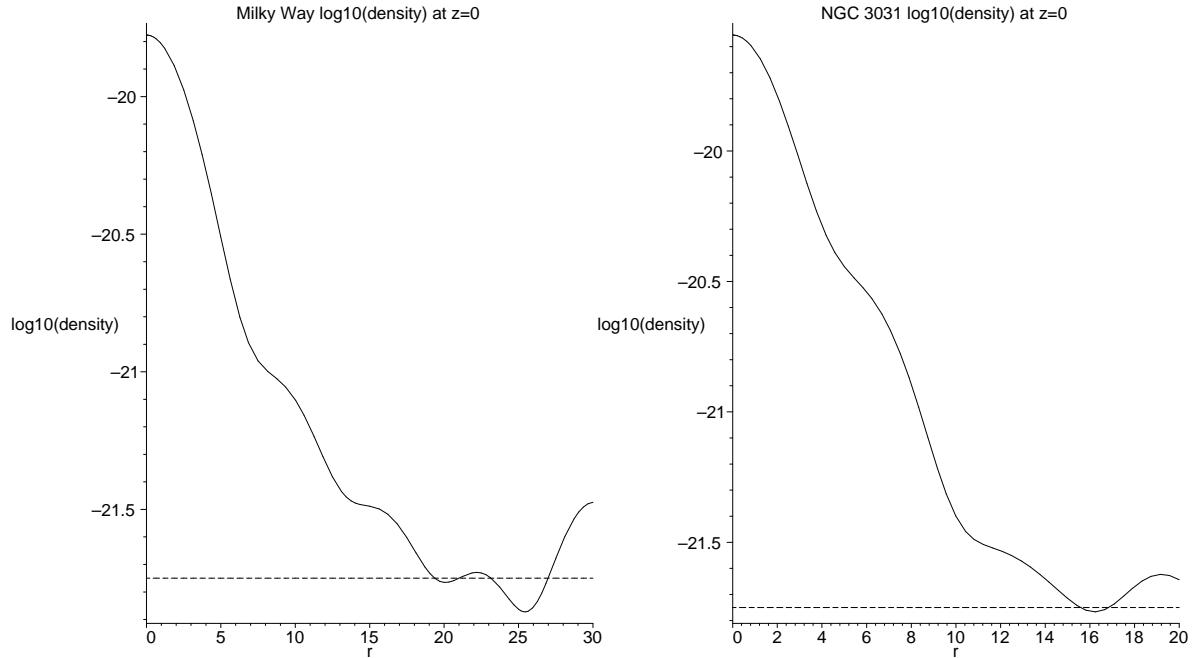


Figure 6: Log graphs of density for the Milky Way (left) and NGC 3031 (right) showing the density fall-off. The -21.75 dashed line provides a tool to predict the outer limits of visible matter. The fluctuations at the end are the result of limited curve-fitting terms.

(with Newtonian dynamics) by Kent [9] of $15.1 \times 10^{10} M_{\odot}$. While the visible light profile terminates at $r = 14$ Kpc, the HI profile extends to 30 Kpc. If the density is integrated to 14 Kpc, it yields a mass-to-light ratio of $7Y_{\odot}$. However, integrating through the HI outer region to $r = 30$ Kpc yields $14Y_{\odot}$ using data from [10].

For NGC 7331, we calculate a mass of $26.0 \times 10^{10} M_{\odot}$. Kent [9] finds a value of $43.3 \times 10^{10} M_{\odot}$. For NGC 3031, the mass is calculated to be $10.9 \times 10^{10} M_{\odot}$ as compared to Kent's value of $13.3 \times 10^{10} M_{\odot}$. Our masses are consistently lower than the masses projected by models invoking dark matter halos and our distributions roughly tend to follow the contours of the optical disks.

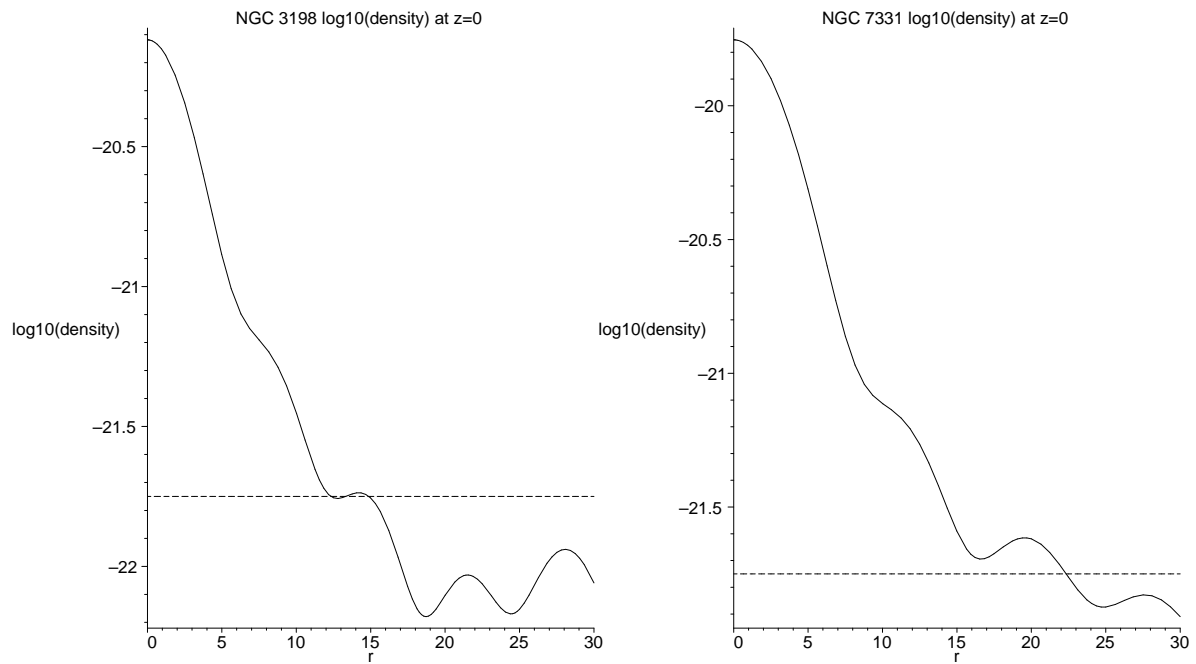


Figure 7: Log graphs of density for the NGC 3198 (left) and NGC 7331 (right) showing the density fall-off. The -21.75 dashed line provides a tool to predict the limits of luminous matter. As before, there are fluctuations near the border.

It is interesting to note that from the figures provided by Kent [9] for optical intensity curves and our log density profiles for NGC 3031, NGC 3198 and NGC 7331, we determine that the threshold for the onset of visible galactic light is at $10^{-21.75} \text{ kg}\cdot\text{m}^{-3}$ (Figure 6 and Figure 7). It would be of interest to explore as many sources as possible to test the indicated hypothesis that this density is the universal optical luminosity threshold for galaxies. Alternatively, should this hypothesis be further substantiated, the radius at which the optical luminosity fall-off occurs can be predicted for other sources using this special density parameter. The predicted optical luminosity fall-off for the Milky Way is at a radius of 19-21 Kpc based upon the density threshold that we have determined.

Various authors attempt to incorporate the Tully- Fisher law [14] into their modified theories of gravity. General relativity can provide an equivalent albeit considerably more complicated relation but in integral form. From (11) and (15), the radial gradient of the galactic mass can be expressed in terms of velocity as

$$M_r(r) = \frac{1}{2G} \int_0^\infty \left(r (V_r^2 + V_z^2) + \frac{V^2}{r} + 2VV_r \right) dz \quad (19)$$

and a doubling has been used to account for the lower disk contribution.

4 Concluding Comments

One might be inclined to question how this large departure from the Newtonian picture regarding galactic rotation curves could have arisen since the planetary motion problem is also a gravitationally bound system and the deviations there using general relativity are so small. The reason is that the two problems are very different: in the planetary problem, the source of gravity is the sun and the planets are treated as test particles in

this field (apart from contributing minor perturbations when necessary). They respond to the field of the sun but they do *not* contribute to the field. By contrast, in the galaxy problem, the source of the field is the combined rotating mass of all of the freely-gravitating elements themselves that compose the galaxy.

We have seen that the non-linearity for the computation of density inherent in the Einstein field equations for a stationary axially-symmetric pressure-free mass distribution, even in the case of weak fields, leads to the correct galactic velocity curves as opposed to the incorrect curves that had been derived on the basis of Newtonian gravitational theory. Indeed the results were consistent with the observations of velocity as a function of radius plotted as a rise followed by an essentially flat extended region and no halo of exotic dark matter was required to achieve them. The density distribution that is revealed thereby is one of a concentrated mass-density disk, in support of the “maximum disk” (see [11] and references therein) models but without an accompanying extended dark matter halo. With the “dark” matter concentrated in the disk which is itself visible, it is natural to regard the non-luminous material as normal baryonic matter.

It is unknown how far the galactic disks extend. More data points beyond those provided thus far by observational astronomers would enable us to extend the velocity curves further. Presumably a point (let us call it r_f) is reached where we can set ρ to zero. At this point, (2) no longer applies as there are no longer co-rotating fluid elements being tracked. As a result, (9) no longer applies and the w function is no longer constant. Beyond r_f , no further mass is accumulated. If we suppose that this is the case at the extremities of the HI regions indicated, then the masses that we have derived are indeed

the total masses. *It is to be emphasized that the flat rotation curves have been achieved with these modest mass values, without a massive exotic dark matter halo.*

Nature is merciful in providing one linear equation that enables us by superposition to model disks of variable density distributions. This opens the way to studies of other sources and with further refinements. Moreover, it will be of interest to extend this general relativistic approach to the other relevant areas of astrophysics with the aim of determining whether there is any scope remaining for the presence of any exotic dark matter in the universe. Clearly the absence of such exotic dark matter would have considerable significance.

Acknowledgments: This work was supported in part by a grant from the Natural Sciences and Engineering Research Council of Canada.

References

- [1] Binney, J. and Tremaine, S., 1987. *Galactic Dynamics* Princeton University Press, Princeton, N.J.
- [2] Mestel, L., 1963. *Mon. Not. Roy. Astron. Soc.* **126**, 553.
- [3] Milgrom, M., 1983. *Ap. J.* **270**, 365; *ibid.* 1986. **302**, 617; *ibid.* with Bekenstein, J.D., 1984. **286**, 7; Bekenstein, J.D., 1990. *Developments in General Relativity, Astrophysics and Quantum Theory*. Eds. F.I. Cooperstock, L.P. Horwitz and J. Rosen. IOP Publishing Ltd, Bristol, England; Brownstein, J.R. and Moffat, J.W., astro-ph/0506370.
- [4] Keeton, Charles R., 2001. *Ap. J.* **561**, 46.
- [5] Winicour, J., 1975. *J. Math. Phys.* **16** , 1805.
- [6] van Stockum, W.J., 1937. *Proc. R. Soc. Edin.* **57**, 135.
- [7] Bonnor, W.B., 1977. *J. Phys. A: Math. Gen.* **10**, 1673.
- [8] Ford, L.B., 1955. *Differential Equations* McGraw-Hill, New York.
- [9] Kent, S.M., 1987. *Astron. J.* **93**, 816.
- [10] van Albada, T.S., Bahcall, J.N., Begeman, K. and Sancisi, R., 1985. *Ap. J.* **295**, 305.
- [11] Bosma, A., 2002. *The Dynamics, Structure and History of Galaxies, ASP Conference Series* Eds. G.S. DaCosta and E.M. Sadler astro-ph/0312154; Bosma, A. 2003 *Dark Matter in Galaxies, IAU Symp., Vol. 220* Eds. S. Ryder, D.J. Pisano, M. Walker and K.C. Freeman, astro-ph/0112080.

- [12] Cooperstock, F.I., Jhingan, S., Joshi, P.S. and Singh, T.P. 1997. *Class. Quantum Grav.* **14**, 2195.
- [13] Clewley, L. et al, astro-ph/0310675; Wilkinson, M. and Evans, N. 1999. *MNRAS* **310**, 645.
- [14] Tully, R.B. and Fisher, J.R., 1977. *Astronomy and Astrophysics* **54**, 661.

5 Appendix

The coefficients for

$$N(r, z) = - \sum_{n=1}^{10} C_n k_n e^{-k_n |z|} J_1(k_n r)$$

are tabulated in Tables 1 to 4 with r and z in Kpc. The velocity in m/sec is given by

$$V(r, z) = \frac{3 \times 10^8}{r} N(r, z)$$

and the density in kg/m^3 is given by

$$\rho(r, z) = 5.64 \times 10^{-14} \frac{(N_r^2 + N_z^2)}{r^2}$$

$-C_n k_n$	k_n
0.0012636497740	0.06870930165
0.0004520156256	0.15771651740
0.0001785404942	0.24724936890
0.0002946610499	0.33690098400
0.0000103378815	0.42659764880
0.0002127633340	0.51631611340
-0.0000221015927	0.60604676080
0.0001346275993	0.69578490080
-0.0000123824930	0.78552797510
0.0000666973093	0.87527447050

Table 1: Curve-fitted coefficients for the Milky Way

$-C_n k_n$	k_n
0.0011694103480	0.1093102526
0.0004356556836	0.2509126413
0.0003677376760	0.3933512687
0.0001484103801	0.5359788381
0.0000837048346	0.6786780777
0.0000414084713	0.8214119986
0.0000429277032	0.9641653013
0.0000550130755	1.1069305240
0.0000238560073	1.2497035970
0.0000129841761	1.3924821120

Table 2: Curve-fitted coefficients for NGC 3031

$-C_n k_n$	k_n
0.00093352334660	0.07515079869
0.00020761839560	0.17250244090
0.00022878035710	0.27042899730
0.00009325578799	0.3684854512
0.00007945062639	0.4665911784
0.00006081834319	0.5647207491
0.00003242780880	0.6628636447
0.00003006457058	0.7610147353
0.00001687931928	0.8591712228
0.00003651365250	0.9573314522

Table 3: Curve-fitted coefficients for NGC 3198

$-C_n k_n$	k_n
0.0015071991080	0.0586542819
0.0003090462519	0.1346360514
0.0003960391396	0.2110665344
0.0001912008955	0.2875984009
0.0002161444650	0.3641687246
0.0000988404542	0.4407576578
0.0001046496277	0.5173569909
0.0000619051218	0.5939627202
0.0000647087250	0.6705726616
0.0000457420923	0.7471855236

Table 4: Curve-fitted coefficients for NGC 7331